Blind detection of an elliptically polarized wave in three-component seismic measurement

Koji NAGANO
Muroran Institute of Technology, nagano@csse.muroran-it.ac.jp
Muroran, Hokkaido, 050-8585, Japan

ABSTRACT

Duration of an elliptically polarized wave is detected by using the blind signal separation and the cross-correlation analysis in three-component seismic signals. Observed three-component signals are assumed to be linear combinations of the elliptically polarized wave and another wave. The fourth-order cumulant, kurtosis, is used to measure a degree of the independence of the transformed signals. To actually minimize or maximize the kurtosis, a fixed-point algorithm is employed. Duration of the polarized wave is detected by analyzing the cross-correlations between the $\pi/2$ phase-shifted signal and the zero phase-shifted signal. The duration of crack-waves which have the elliptical particle motion is detected well by using the algorithm.

1 Introduction

Three-component (3C) seismic measurement is employed in geophysical exploration because three-dimensional particle motions of the seismic waves have a lot of important information about the subsurface medium. Each mode of the seismic waves has its characteristic particle motion. Identification of the particle motion is important to get the information and suppress noise. Therefore, analyzing techniques of the particle motion is important in the seismic measurement.

Lacoume et al. [1] described blind separation of the polarized waves. They analyzed two-component signals to separate a Rayleigh wave, which has an elliptical particle motion, from a compressional wave. Their method can be applied to restricted seismic data because their method was made for two-component data. The performance of the separation depends on a relation between direction of a 2C seismic detector and orientation of the polarization ellipse formed by the Rayleigh wave.

I describe an algorithm to detect duration of the seismic waves with the elliptical particle motion in the 3C seismic signal. The algorithm consists of the blind separation using the independent component analysis, which uses a contrast function of the fourth order cumulant, and cross-correlation analysis between $\pi/2$ and zero phase-shifted signals. The algorithm can be used in any direction of the 3C seismic detector. The detection algorithm is illustrated using crack-waves, which have the elliptical particle motion. The duration of the crack-waves is detected well with the algorithm.

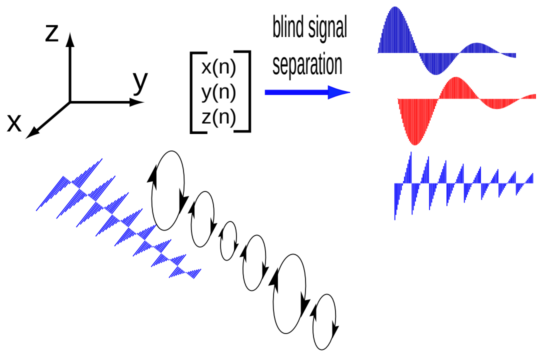

Figure 1: The blind signal separation of the elliptically polarized wave in the three-component detector.

2 Model of blind detection

A statistical model is assumed for the algorithm of the blind detection in the 3C seismic signal. Figure 1 shows a concept of the blind signal separation of the waves including the elliptically polarization. The 3C signal is observed in the 3C seismic measurement in which three seismic sensors are installed to be perpendicular to each other. A seismic wave with the elliptical particle motion and another seismic wave are simultaneously mixed and observed in the 3C signal. Duration of the wave with the elliptical particle motion is estimated using only the observed 3C signal. No assumptions on a transfer function of the 3C detector are used in the detection procedure. True waveforms of the waves are not identified. Therefore, I call this detection problem "blind detection."

We observe three scalar random variables x_1, x_2, x_3 which are assumed to be linear combinations of three unknown independent components s_1, s_2, s_3 that are mutually statistically independent, and zero-mean. The original variables are non-Gaussian. It is convenient to use vector-matrix notation. We denote the observed variables x_1, x_2, x_3 by $\boldsymbol{x}$ and the original variables s_1, s_2, s_3 by $\boldsymbol{s}$. Using these vector notation, the linear mixture model is written as

$$\boldsymbol{x} = \boldsymbol{A}\boldsymbol{s}, \tag{1}$$

where $\boldsymbol{A}$ is an unknown 3×3 mixing matrix with real components. All vectors are understood as column vectors.

The three-component variables represent the particle motion associated with seismic waves in the 3C seismic measurement. A wave with the elliptical particle motion is represented in two components in the original variables because axes of the elliptical particle motion are orthogonal. Let us assume that another wave arrives together with this elliptically polarized wave in the 3C seismic detector. Orientation of the polarization ellipse has no relation with the axes of the sensors. Therefore, this statistical model represented in (1) has no restriction to use in the detection of the elliptically polarized wave in the 3C seismic measurement.

The wave with the elliptical particle motion can be represented in two components of $\boldsymbol{s}$. The two components which represent the elliptical particle motion are statistically independent because probability distributions of the two components have no relation with each other. Another seismic wave is also statistically independent to the waves which represent the elliptical particle motion.

3 Algorithm of blind detection

The first step of the blind detection is the blind signal separation using independent component analysis (ICA) [2] and the second step is the cross-correlation analysis of the signal transformed by the blind signal separation. Number of the waves except for the elliptically polarized wave is more than one in many cases of the real seismic measurements. Such signals do not satisfy the model of (1). Therefore, I add the cross-correlation analysis to the blind signal separation to detect the duration of the elliptically polarized wave.

The observed signal $\boldsymbol{x}$ is transformed to $\boldsymbol{y}$ by a matrix $\boldsymbol{W}^T$ in the blind separation,

$$\boldsymbol{y} = \boldsymbol{W}^T\boldsymbol{x}, \tag{2}$$

where ^{T} denotes the transpose. Two ambiguities of both scale and permutation are held in the blind separation. Therefore, the transform matrix $\boldsymbol{W}^T$ and the mixing matrix $\boldsymbol{A}$ are represented by a permutation matrix $\boldsymbol{P}$ and a diagonal matrix $\boldsymbol{D}$ in

$$\boldsymbol{W}^T\boldsymbol{A} = \boldsymbol{P}\boldsymbol{D} \neq \boldsymbol{I}, \tag{3}$$

where $\boldsymbol{I}$ is an unit matrix.

The transform matrix $\boldsymbol{W}^T$ is obtained so that the components y_1, y_2, y_3 can be statistically independent

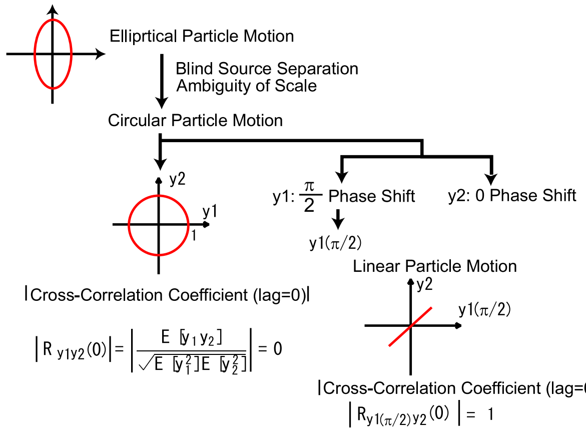

Figure 2: Detection method of elliptically polarized particle motion.

to one another. $\boldsymbol{x}$ is centered to simplify the algorithm. I use the fixed-point algorithm to get the statistically independent signal $\boldsymbol{y}$ after whitening [3]. The eigenvalue decomposition of a covariance matrix $E\left[\boldsymbol{x}\boldsymbol{x}^T\right] = \boldsymbol{U}\Lambda\boldsymbol{U}^T$ is used to whiten $\boldsymbol{x}$. The whitened signal $\tilde{\boldsymbol{x}}$ is represented by

$$\tilde{\boldsymbol{x}} = \Lambda^{-\frac{1}{2}}\boldsymbol{U}^T\boldsymbol{x}. \tag{4}$$

After the whitening, an orthogonal matrix $\boldsymbol{R}^T$ is used to get the statistically independent signal $\boldsymbol{y}$,

$$\boldsymbol{y} = \boldsymbol{R}^T\tilde{\boldsymbol{x}}. \tag{5}$$

$\boldsymbol{R}^T$ is obtained so that a contrast function of the statistical independence between the components of the transformed signal $\boldsymbol{y}$ should be maximum or minimum. I use the fourth order cumulant with zero lag, kurtosis, as the contrast function. The contrast function $\phi\left(\boldsymbol{r}_i^T\right)$ is represented by

$$\begin{aligned}\phi\left(\boldsymbol{r}_i^T\right) &= E\left[y_i^4\right] - 3\left\{E\left[y_i^2\right]\right\}^2 \\ &= E\left[\left(\boldsymbol{r}_i^T\,\tilde{\boldsymbol{x}}\right)^4\right] - 3\left\{E\left[\left(\boldsymbol{r}_i^T\,\tilde{\boldsymbol{x}}\right)^2\right]\right\}^2,\end{aligned} \tag{6}$$

where $\boldsymbol{r}_i$ is the i th column vector of $\boldsymbol{R}$. When $\phi\left(\boldsymbol{r}_i^T\right)$ is maximum or minimum under a condition of $\|\boldsymbol{r}_i^T\| = 1$, the transformed signal $\boldsymbol{y}$ equals to $\pm\boldsymbol{s}$. Finally the transformation is represented by

$$\boldsymbol{y} = \boldsymbol{R}^T\Lambda^{-\frac{1}{2}}\boldsymbol{U}^T\boldsymbol{x}. \tag{7}$$

Variances of the components in $\boldsymbol{y}$, transformed by (7), equal unity. Therefore, a circular particle motion is obtained in (7) when there is the elliptical particle motion. The circular particle motion can be decomposed to two oscillations which have a phase delay of $\pi/2$. Axes of the two oscillations are orthogonal. A zero-lag cross-correlation coefficient of the two components which show the circular particle motion is equal to zero. If the phase

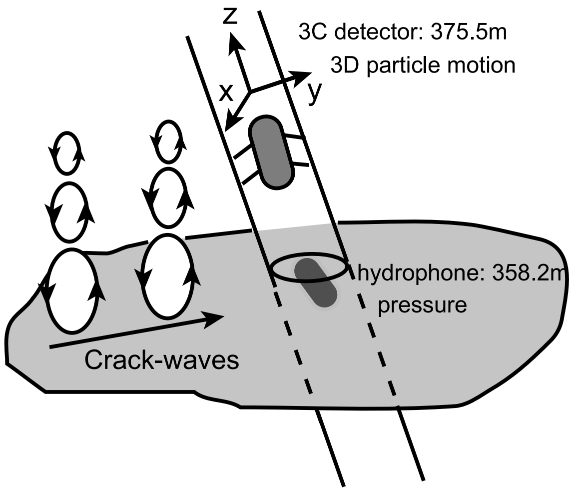

Figure 3: Measurement of crack-waves with a 3C seismic detector and a hydrophone. The crack-waves propagate along a crack. Their particle motion is ellipse and perpendicular to the crack surface.

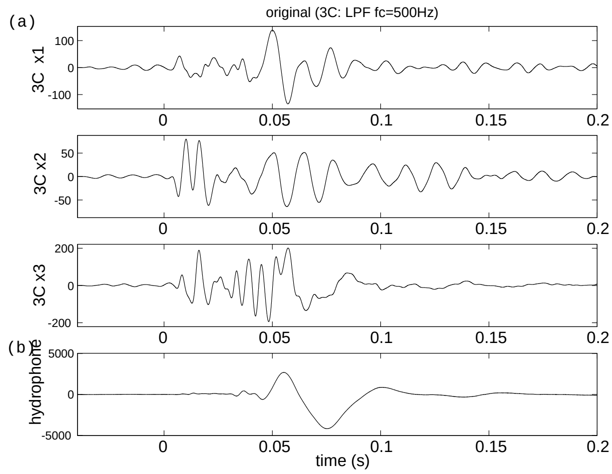

Figure 4: Waveforms detected in the crack-waves measurement. (a) Low-pass filtered waveforms detected with the 3C seismic detector. $f_c = 500$ Hz. It is difficult to determine the arrival of the crack-waves. (b) Waveform detected with the hydrophone. Tube wave analysis indicated that the large waves at the time of 0.05 s were the crack-waves.

of a component in the circular particle motion is shifted by $\pi/2$ and another component is zero-phase shifted, the circular particle motion becomes a linear particle motion. The linear particle motion shows that an absolute value of the zero-lag cross-correlation coefficient is equal to unity. A random particle motions also show that the zero-lag cross-correlation coefficient is zero. The zero-lag cross-correlation coefficient between $\pi/2$ and zero phase-shifted signals does not equal unity in the random particle motion. Figure 2 shows the relation between the particle motions and their cross-correlation coefficients.

Cross-correlation coefficient at time t is produced multiplying the signal by a rectangular window function centered at t. The zero-lag cross-correlation coefficient of the transformed components y_i and y_j at t is represented by $R_{y_i y_j}(t, 0)$. The zero-lag cross-correlation coefficient of the $\pi/2$ and zero phase-shifted components at t is also represented by $R_{y_i\left(\frac{\pi}{2}\right)y_j}(t, 0)$. The duration of the wave with the elliptical particle motion is found by a detection function $C(t)$,

$$C(t) = |R_{y_i\left(\frac{\pi}{2}\right)y_j}(t, 0)| - |R_{y_i y_j}(t, 0)|. \qquad (8)$$

I analyze three combinations (y_1, y_2), (y_1, y_3), and (y_2, y_3) in (8) because of the ambiguity of the permutation. $C(t)$ is close to unity when there is the elliptical particle motion.

4 Blind detection of crack-waves

I apply the described algorithm to a data of crack-waves. The crack-waves are one of elastic surface waves, e.g., the Rayleigh waves. They propagate along a crack and their particle motion is an ellipse perpendicular to the crack surface. Orientation of the crack surface can be estimated from the particle motion of the crack-waves [4].

Figure 3 illustrates a concept of a crack-wave measurement using a 3C seismic detector and a hydrophone. The 3C seismic detector measures the three-dimensional particle motion associated with seismic waves, and the hydrophone measures pressure waves in water in the crack.

Crack-waves were measured at Higashi-Hachimantai hot dry rock model field, Japan [5]. There is an artificial subsurface fracture at a depth of 370 m. An intersection depth of a borehole is 358.2 m. A downhole air gun was used as a wave source. The crack-waves can be detected at the intersection of the borehole and the fracture. The hydrophone was suspended at a depth of 358.2 m and the 3C seismic detector was fixed on a borehole wall at a depth of 357.5 m. Velocity of the crack-waves is almost 100 m/s [5]. The velocities of compressional and shear waves of intact rock in this field are 3100 m/s and 1860 m/s, respectively.

Figure 4 shows waveforms detected with the 3C seismic detector and the hydrophone. The 3C signal detected with the 3C seismic detector is filtered to suppress high frequency components at a cut-off frequency of 500 Hz. The hydrophone is better than the 3C seismic detector to determine the arrival of the crack-waves because energy of the crack-waves concentrates in a water layer in a fracture. The crack-waves convert to tube waves at the intersection with the borehole. Tube wave analysis indicated that the waves with a large amplitude at 0.05 s in Figure 4 (d) are the crack-waves [5]. On the other hand, the energy of the crack-waves in rock layers

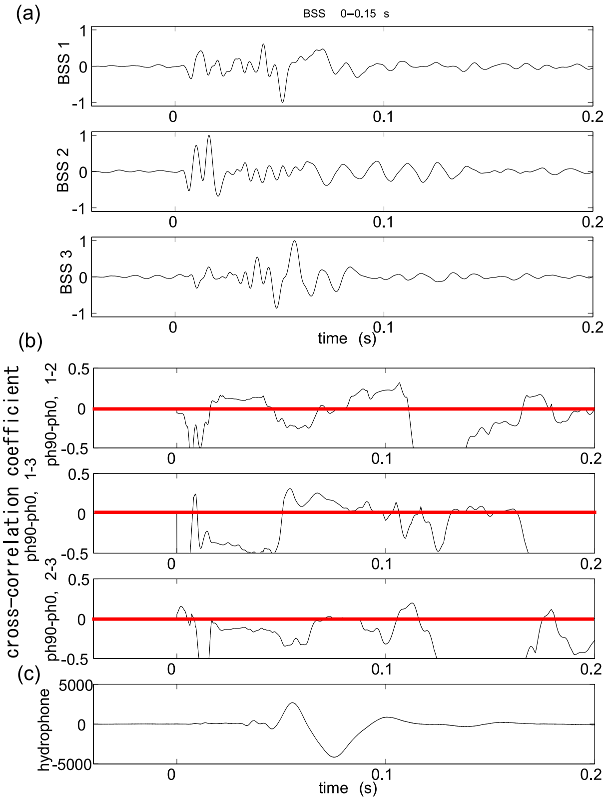

Figure 5: The cross-correlation analysis of the blind separated waves. (a) Waveforms after the blind separation. (b) Differences of absolute values between the cross-correlation coefficients with zero phase-shifted signals and that with $\pi/2$ phase-shifted signals. Data length to calculate the cross-correlation is 0.04 s. (c) The waveform detected with the hydrophone. The crack-waves arrive at 0.05 s.

is less than that in the water, and the energy of the compressional and shear waves in the rock layers is larger than that in the water layer. The 3C seismic detector detects the particle motion of the rock layer. Therefore, the other seismic waves were detected before the arrivals of the crack-waves in Figure 4 (a)-(c). These waves make it difficult to detect the crack-waves in the signal detected with the 3C seismic detector.

I apply the described algorithm of the blind detection of the elliptical particle motion to the data containing the crack-waves. Figure 5 (a) shows a result of the blind separation. The waveform data from 0 s to 0.15 s in Figure 4 (a)-(c) is used to calculate the transform matrix $\boldsymbol{W}^T$. Figure 5 (b) shows $C(t)$ to detect the wave with the elliptical particle motion. Length of the window function for the calculation of the cross-correlation is 0.04 s. This length has a relation with time resolution to detect the wave. $C(t)$ is larger than zero from 0.05 s to 0.09 s in the middle graph of Figure 5 (b). This duration is identified to that of the crack-waves in Figure 5 (c). Other durations with positive values in Figure 5 (a) and (c) are short to identify as the elliptical particle motion because of the time resolution.

Only one wave except for the elliptically polarized wave is assumed in the model described in section 2. There are the compressional and shear waves in advance to the crack-waves. Other modes which are generated from these waves arrive if there are boundaries in the medium. This deviation from the model affects the result of the blind separation. It is difficult to determine the duration of the crack-waves in Figure 5 (a). Therefore, the cross-correlation analysis, which helps the blind separation, is necessary to detect the duration.

5 Conclusion

I have shown that the combination of the blind separation using kurtosis and the cross-correlation analysis can estimate the duration of the waves with the elliptical particle motion using the real data, the crack-waves. The number of the waves in the crack-waves is more than that in the model. The cross-correlation analysis can achieve the detection of the duration. The waveforms are not, however, identified. This result has potentials to detect other characteristic polarizations, e.g., linear polarization, in the 3C seismic measurement.

Acknowledgments: I thank Nicolas Le Bihan, LIS, INPG, for his discussion on the higher-order statistics. This study was supported by the Ministry of Education, Culture, Sports, Science, and Technology, Grant-in-aid for Scientific Research (C), 13650980, 2001 and Toyota High-tech Research Grant Program.

References

[1] Lacoume, J.L., F. Glangeaud, and J. Mars, "Blind separation of polarised waves," *EUSIPCO*, 1629-1632, 1998.

[2] Hyvärine, A. and E. Oja, "Independent component analysis: algorithms and applications," *Neural Networks*, **13**, 411-430, 2000.

[3] Hyvärine, A. and E. Oja, "A fast fixed-point algorithm for independent component analysis," *Neural Computation*, **9**, 1483-1492, 1997.

[4] Nagano, K., K. Sato, and H. Niitsuma, "Polarization of crack waves along an artificial subsurface fracture," *Geophysical Research Letters,* **23**, 2017-2020, 1996.

[5] Nagano, K. and H. Niitsuma, "Dispersion analysis of crack-caves in an artificial subsurface fracture using two crack models," *IEEE Transaction on Geoscience and Remote Sensing*, **38**, 3-11, 2000.